Journal of Intensive Medicine 5 (2025) 79–88

Contents lists available at ScienceDirect

Journal of Intensive Medicine

journal homepage: www.elsevier.com/locate/jointm

Original Article

Intestine-derived fibroblast growth factor 19 alleviates lipopolysaccharide-induced liver injury by regulating bile acid homeostasis and directly improving oxidative stress

Xiaomeng Tang[1,2,#], Jingjing Ning[1,2,#], Yilin Zhao[1,2], Shuyun Feng[1,2], Lujing Shao[1,2], Tiantian Liu[1,2], Huijie Miao[1,2,3], Yucai Zhang[1,2,3,*], Chunxia Wang[1,2,3,*]

[1] *Department of Critical Care Medicine, Shanghai Children's Hospital, School of Medicine, Shanghai Jiao Tong University, Shanghai, China*
[2] *Laboratory of Critical Care Translational Medicine, Institute of Pediatric Infection, Immunity, and Critical Care Medicine, Shanghai Children's Hospital, Shanghai Jiao Tong University School of Medicine, Shanghai, China*
[3] *Institute of Pediatric Critical Care, Shanghai Jiao Tong University, Shanghai, China*

ARTICLE INFO

Managing Editor: Jingling Bao/ Zhiyu Wang

Keywords:
FGF19
Bile acid
Oxidative stress
Mitochondria dysfunction
Acute liver injury
Sepsis

ABSTRACT

Background: Cholestasis plays a critical role in sepsis-associated liver injury (SALI). Intestine-derived fibroblast growth factor 19 (FGF19) is a key regulator for bile acid homeostasis. However, the roles and underlying mechanisms of FGF19 in SALI are still unclear.

Methods: We conducted a case–control study that included 58 pediatric patients aged from 1 month to 14-years-old diagnosed with sepsis at Shanghai Children's Hospital from January to December 2018 and 30 healthy individuals. The serum FGF19 levels of these patients with sepsis were analyzed and compared with those of healthy controls. Recombinant human FGF19 was intravenously injected in mice once a day for 7 days at a dose of 0.1 mg/kg body weight before lipopolysaccharide (LPS) treatment. Liver bile acid profiles and the gene expression involved in bile acid homeostasis were investigated in the mice groups. Metabolomic data were further integrated and analyzed using Ingenuity Pathways Analysis (IPA) software. In the *in vitro* analysis using HepG2 cells, the influence of FGF19 pretreatment on reactive oxygen species (ROS) production and mitochondrial dysfunction was analyzed. Compound C (CC), an inhibitor of AMP-activated protein kinase (AMPK) activation, was used to confirm the roles of AMPK activation in FGF19-mediated hepatoprotective effects.

Results: Serum FGF19 levels were significantly lower in children with sepsis than in healthy controls (115 pg/mL *vs*. 79 pg/mL, P=0.03). Pre-administration of recombinant human FGF19 alleviated LPS-induced acute liver injury (ALI) and improved LPS-induced cholestasis in mice. Moreover, FGF19 directly reversed LPS-induced intracellular ROS generation and LPS-decreased mitochondrial membrane potential *in vitro* and *in vivo*, resulting in hepatoprotection against LPS-induced apoptosis. More importantly, the inhibition of AMPK activity partially blocked the protective effects of FGF19 against LPS-induced oxidative stress and mitochondrial dysfunction.

Conclusions: Intestine-derived FGF19 alleviates LPS-induced ALI via improving bile acid homeostasis and directly suppressing ROS production via activating the AMPK signaling pathway.

Introduction

Sepsis is defined as life-threatening organ dysfunction caused by a dysregulated host response to infection and is one of the main causes for mortality in patients admitted to the intensive care unit (ICU).[1] Apart from defending the body during an infection, the liver is also the direct target organ of inflammatory injury during sepsis. Significantly, the mortality rate of patients with sepsis-associated liver injury (SALI) ranges from 54% to 68%, which is significantly higher than that in septic patients without liver injury.[2] Therefore, prevention of SALI could be an additional potential strategy for improving sepsis outcome. A specific and effective therapy for preventing SALI could be crucial for the prognosis of sepsis.

* Corresponding authors: Yucai Zhang and Chunxia Wang, Department of Critical Care Medicine, Shanghai Children's Hospital, School of Medicine, No. 355 Luding Road Putuo District, Shanghai Jiao Tong University, Shanghai 20000, China.
E-mail addresses: zyucai2018@163.com (Y. Zhang), karencx0465@163.com (C. Wang).
# Xiaomeng Tang and Jingjing Ning contributed equally to this work.

https://doi.org/10.1016/j.jointm.2024.06.003
Received 14 January 2024; Received in revised form 17 May 2024; Accepted 11 June 2024
Available online 10 October 2024

Cholestasis is one of the main pathological mechanisms underlying SALI. Intrahepatic cholestasis activates inflammation and oxidative stress, leading to apoptosis or necrosis of hepatocytes.[3] During sepsis, the disturbance of bile acid enterohepatic circulation promotes bacterial translocation and endotoxin absorption in the intestine and forms a vicious circle.[4,5] Under normal conditions, bile acids bind to the farnesoid X receptor (FXR) and promote the secretion of fibroblast growth factor 15/19 (FGF15 [mouse]/19 [human]) in the intestine. FGF15/19 is transported to the liver via the portal vein and interacts with the fibroblast growth factor receptor 4 (FGFR4)/β-Klotho dimer in hepatocytes to suppress the expression of cholesterol 7-α-hydroxylase (CYP7A1), leading to bile acid homeostasis.[6–8] In patients with sepsis, the normal feedback inhibition of CYP7A1 transcription by bile acid is impaired, which in turn leads to increased levels of bile acids in the liver.[9,10] More importantly, cholestasis destroys the balance between pro-oxidation and antioxidants, leading to lipid peroxidation and liver damage.[11] In patients with obstructive cholestasis, elevated levels of the oxidative stress marker malondialdehyde (MDA) and reduced levels of glutathione (GSH) are associated with increased levels of alanine aminotransferase (ALT), alkaline phosphatase (ALP), and total bilirubin (TBIL).[12] In addition, reactive oxygen species (ROS) produced by inflammatory cells leads to the diffusion of oxidants into target cells and produces intracellular oxidant stress in target cells.[13] Furthermore, oxidative stress leads to mitochondrial dysfunction, which eventually triggers the necrosis of cells and tissues.[13,14] Recent studies have indicated that FGF19 promotes mitochondrial biosynthesis and antioxidant response and reduces production of ROS.[15,16] FGF19 pretreatment significantly reduces the apoptosis of colon epithelial cells induced by hydrogen peroxide (H_2O_2).[17] These results suggest that in addition to bile acids homeostasis, FGF19 also likely directly regulates antioxidant capacity.

To date, the role and underlying mechanisms of FGF15/19 in SALI have not been reported. To further investigate whether FGF15/19 can alleviate lipopolysaccharide (LPS)-induced acute liver injury (ALI) and elucidate its specific mechanisms, we conducted the experimental study.

Methods

Study approval

A total of 58 children diagnosed with sepsis at Shanghai Children's Hospital from January to December 2018 were included in this study, along with 30 healthy individuals as controls. Sera were collected from sepsis patients at the time of admission to the pediatric intensive care unit (PICU). The residual blood samples from healthy children after routine physical examination were utilized for comparison.

This research study was approved by the Ethics Committee of Children's Hospital affiliated to Shanghai Jiao Tong University (approval number: 2018R039-F01) and was carried out in accordance with the tenets of the Declaration of Helsinki. The informed consent form was signed by the parents or legal guardians of the patients. The inclusion and exclusion criteria of patients and detailed methods can be found in the Supplementary Material.

Animal experiments

In all, 24 male C57BL/6 mice (8–12 weeks old) were bought from the Shanghai Lab, Animal Research Center (Shanghai, China). The mice were exposed to a standard 12-h light/dark cycle and had *ad libitum* access to chow and water. The animals were cared for according to the Ethics Committee guidelines of Shanghai Jiao Tong University Affiliated Children's Hospital (approval number: 2,018,014). To investigate the protective function of FGF19 on LPS-induced ALI, mice were randomly separated into four groups as follows: control (Control), LPS treatment (LPS), FGF19 pretreatment (FGF19), and pretreatment with FGF19 followed by LPS administration (LPS + FGF19). The specific treatment methods for each group are as follows: Control group (n=6): Normal phosphate buffered saline (PBS) in a volume equivalent to the following drug FGF19 was administered via intravenous injection for 7 days, followed by intraperitoneal injection of normal PBS in a volume equivalent to the following drug LPS on the eighth day; LPS group (n=6): PBS was administered via intravenous injection for 7 days, followed by intraperitoneal injection of LPS (5.0 mg/kg body weight, L2630, *Escherichia coli* O111:B4, Sigma-Aldrich, St. Louis, Missouri, USA) on the eighth day for 24 h to induce ALI; FGF19 group (n=6): Recombinant human FGF19 (Novoprotein, Suzhou, Jiangsu, China) was administered via intravenous injection (0.1 mg/kg body weight) for 7 days, followed by intraperitoneal injection of PBS on the eighth day; LPS + FGF19 group (n=6): FGF19 was administered via intravenous injection (0.1 mg/kg body weight) for 7 days, followed by intraperitoneal injection of LPS on the eighth day for 24 h to induce ALI.

On the ninth day, anesthetize the mice using sodium pentobarbital at a dose of 60 mg/kg, administered via intraperitoneal injection. Then the blood was collected from the eyeball, centrifuged to obtain the supernatant, and stored at −80 ˚C for cytokine analysis. Carefully lift the liver tissues with forceps, cut out about 10 mg of tissue, and immediately freeze it in liquid nitrogen. Store the excised tissue temporarily at −80 ˚C.

Analysis of bile acids profiles in the livers of mice

We conducted metabolomics analysis of mouse livers (n = 5) with the Q300 Kit (Metabo-Profile, Shanghai, China). Details are described in the Supplementary Material. The annotated metabolites were mapped to the Ingenuity Pathway Analysis (IPA) database; then, the up-down relationships between metabolites were analyzed based on literature data to finally identify the potential metabolic pathways.

Detection of biochemical indicators of serum in mice

The Hitachi 7180 automatic biochemical analyzer at Shanghai Children's Hospital was used to detect blood biochemical indicators including aspartate aminotransferase (AST), ALT, and TBIL. An enzyme-linked immunosorbent assay (ELISA) kit (Nanjing Jiancheng Bioengineering Institute, Nanjing, China) was used for the determination of serum interleukin-6 (IL-6) levels.

Histopathology

Liver samples were collected and fixed overnight in 4 % paraformaldehyde at 4 ˚C. The next day, the tissues were embed-

ded in paraffin, and 4-μm-thick sections were obtained on glass slides (LEICA, Wetzlar, Hesse, Germany). Dye tissue sections were stained with hematoxylin and eosin and observed under an optical microscope. The laboratory personnel were blinded to the mice grouping during the experiments.

Quantitative real-time polymerase chain reaction

According to the manufacturer's instructions, TRIzol reagent was utilized for the extraction of total mouse liver RNA (Invitrogen Life Technologies, Carlsbad, CA, USA). Reverse transcription of the extracted total RNA was performed using random primers and M-MLV Reverse Transcriptase (Takara, Otsu, Shiga, Japan). Quantitative real-time polymerase chain reaction was carried out using SYBR Green I Master Mix reagent on the ABI 7500 system (Applied Biosystem, Foster, CA, USA). Supplementary Table 1 lists the primers used. The experimental outcomes were quantified by the $2^{-(\Delta\Delta Ct)}$ method.

Immunohistochemical staining

Liver tissue slices (4-μm-thick) were treated with 3 % hydrogen peroxide (H_2O_2) for 20 min to block endogenous peroxidase activity, then incubated with 1 % bovine serum albumin and anti-phospho-AMPK (#2535, Cell Signaling, Massachusetts, USA, 1:1000) for 2 h. Next, horseradish peroxidase (HRP)-conjugated anti-goat IgG was incubated for 60 min.

Cell culture and treatment

HepG2 cells (HB-8065) were purchased from the Shanghai Institute of Cell Biology (Shanghai, China), and then cultured in Dulbecco's Modified Eagle Medium (DMEM) in 10 % fetal bovine serum (FBS) in a humidified incubator at 37 °C (5 %W CO_2). Control group (n=3): The HepG2 cells were cultured with DMEM in 10% FBS without any other treatment measures and served as the blank control. LPS group (n=3): LPS (40 μg/mL) was used to treat HepG2 cells for 8 h to mimic sepsis-induced hepatocyte injury. FGF19 group (n=3): HepG2 cells were pretreated with human recombinant FGF19 at a dose of 10 ng/mL for 24 h. LPS + FGF19 group (n=3): HepG2 cells were pretreated with FGF19 at a dose of 10 ng/mL for 24 h, followed by LPS treatment for another 8 h.

To study the direct protective functions of FGF19 on oxidative stress, H_2O_2 was used at a dose of 750 μmol/L for 2 h to construct the cell model for oxidative stress. To study the effect of AMP-activated protein kinase (AMPK) activation, AMPK inhibitor Compound C (CC) was used to suppress the AMPK activation. HepG2 cells were pretreated with 10 μmol/L CC for 2 h prior to FGF19 treatment, followed by LPS treatment for another 8 h. All cell culture experiments were repeated in triplicate for each group.

Western blotting

Liver tissue and HepG2 cells were homogenized in RIPA lysis buffer for further analysis (Beyotime Biotechnology, Shanghai, China). Primary antibodies were incubated overnight at 4 °C; these included anti-Caspase 3 (ab13847, Abcam, Cambridge, UK, 1:500); anti- BCL2-Associated X Protein (#5023, Cell Signaling, 1:1000); anti-AMPK (#2532, Cell Signaling, 1:1000); anti-phospho-AMPK (#2535, Cell Signaling, 1:1000); anti-β-actin (#4970, Cell Signaling, 1:1000); and anti-GAPDH (#2118, Cell Signaling, 1:1000).

Peroxidase-conjugated goat anti-rabbit IgG (ZSGB-BIO, Beijing, China) was purchased from Millipore (Bedford, MA, USA), and staining was detected using the enhanced chemiluminescence technique (GE Health Care, Mississauga, Canada). Images were analyzed on a C-Digit chemiluminescent Western blot scanner (LI-COR, Lincoln, USA). ImageJ® image processing program v1.32 (National Institutes of Health, Bethesda, USA) was used to measure the band intensities and normalized to GAPDH.

TdT-mediated dUTP nick-end labeling (TUNEL) staining

HepG2 cells were fixed in 4% paraformaldehyde for 30 min. Then, 0.3% Triton X-100 in PBS was added and incubated at room temperature for 5 min. After washing twice with PBS, TUNEL detection solution was added and incubated at 37 °C for 60 min in the dark. After washing thrice in PBS or Hank's Balanced Salt Solution, a fluorescence microscope was used to visualize the images under an excitation wavelength of 450–500 nm and emission wavelength of 515–565 nm.

Detection of intracellular ROS

HepG2 cells were incubated with ROS-specific fluorescent dye DCFH-DA (Nanjing Jiancheng Bioengineering Institute) at 37 °C for 30 min in the dark. Intracellular ROS was observed under fluorescence microscopy using appropriate filters (excitation wavelength: 485 nm, emission wavelength: 525 nm) according to the manufacturer's instructions and operation manual.

JC-1 staining for detecting mitochondrial membrane potential

Mitochondrial transmembrane potential ($\Delta\psi$m) of HepG2 cells was quantified under fluorescence microscopy with the JC-1 Assay Kit (Beyotime Biotechnology) based on the manufacturer's instructions and operation manual. The ratios of red/green fluorescent densities were analyzed by ImageJ® to quantify the changes of relative $\Delta\psi$m.

Cell viability detection

The ic1000 automatic cell counter (Count star, USA) was used to calculate the HepG2 cells' viability. The viability and the absolute number of cells were recorded and repeated in three different fields for each sample. Finally, the average of three values was used.

Statistical analyses

Normally distributed data were expressed as the mean±standard deviation (SD) or n (%). Non-normally distributed data were statistically described using median (interquartile range). All analyses were conducted by GraphPad Prism version 6.0 (Graph-Pad Software, San Diego, CA, USA). A two-tailed Student's t-test was designed to contrast the distinctions between different groups. One-way analyses of variance or two-way analyses of variance with Bonferroni's *post hoc* correction was used when comparing among greater than

3 or 4 groups. P <0.05 was considered to indicate statistically significant differences.

Results

FGF19 demonstrates hepatoprotective properties against SALI

The baseline characteristics of pediatric patients with sepsis are listed in Supplementary Table 2. Serum FGF19 levels were significantly lower in children with sepsis than in healthy controls (P=0.03). The average serum FGF19 concentration in the control group children and sepsis group children was 115 pg/mL and 79 pg/mL, respectively (Figure 1A).

In animal experiments, the LPS + FGF19 group displaying relived hepatic congestion and hepatic plate disorder and decreased inflammatory cell infiltration and focal necrosis compares to the LPS group (Figure 1B). In addition, the elevated levels of ALT (P=0.0007), AST (P=0.01), IL-6 (P=0.01), and TBIL (P=0.01) in the LPS + FGF19 group mice were decreased compared with the LPS group mice (Figure 1C–F).

The survival rate of HepG2 in the LPS + FGF19 group was higher than in the LPS group (Figure 1G–I). Furthermore, the expression of Caspase 3 in the LPS + FGF19 group was decreased compared to the LPS group (Figure 1J and K).

FGF19 pretreatment improves LPS-induced bile acids disorder in livers

Metabolomics analysis of mouse liver showed changes in the metabolite composition compared to the LPS group, with reductions observed in organic acids and bile acid levels in the LPS + FGF19 group (Figure 2A). The bile acids heatmap and total bile acid (TBA) level analysis from liver bile acid metabolomics showed that FGF19 reversed the LPS-induced increase in both TBA and almost all individual bile acid levels (Figure 2B and C). Moreover, the bile acid profiles in livers were changed considerably in response to LPS, which were partially improved by FGF19 pretreatment (Figure 2D). FGF19 improved the LPS-induced increased bile acids, especially in primary bile acids and conjugated bile acids (Figure 2E and F). After LPS stimulation, the levels of tauro-α-muricholic acid/tauro-β-muricholic acid (TαMCA/TβMCA), tauroursodeoxycholic acid (TUDCA), α-muricholic acid (αMCA), ursodeoxycholic acid (UDCA), tauro-ω-muricholic acid (TωMCA), taurohyodeoxycholic acid (THDCA), and ω-muricholic acid (ωMCA) increased. However, in the LPS + FGF19 group, the levels of these bile acids in the liver, including TαMCA/TβMCA and TUDCA, were reduced, indicating that they were reversed by FGF19 pretreatment (Figure 2G and H).

FGF19 pretreatment suppresses LPS-induced bile acids synthesis and stimulates the expression of bile acids exporter in livers

Further analysis indicated that the mRNA expressions of CYP7A1 and sterol 12α-hydroxylase (CYP8B1) involved in bile acid synthesis were suppressed in livers in the LPS + FGF19 group compared to the LPS group (Figure 3A). In addition, the mRNA expression of apical bile acid exporters including the bile salt export pump (BSEP) and multidrug resistance-associated protein-2 (MRP2), multidrug resistance-associated protein-3 (MRP3), and multidrug resistance-associated protein-4 (MRP4) were decreased in response to LPS stimuli, which were stimulated by FGF19 pretreatment (Figure 3B). The mRNA expressions of the basolateral bile acid uptake transporters, *e.g.*, organic anion transporting polypeptide-4 (OATP4) and sodium taurocholate co-transporting polypeptide (NTCP), were inhibited in mice livers in the LPS group, which was partially alleviated in the LPS + FGF19 group (Figure 3C).

FGF19 alleviates LPS-induced apoptosis associated with AMPK activation in vivo and in vitro

To further illustrate and visualize the potential mechanisms of FGF19 improving the bile acid homeostasis and its association with liver injury in response to LPS, the results of IPA based on metabolomic data showed the top metabolic network, which included 13 molecules in our listed different metabolites, and highlighted a marked connection with bile acid, Fos proto-oncogene, Activator Protein 1 transcription factor subunit (*FOS*), and AMPK (IPA scores: 38, Figure 4A). The activation of phosphorylated AMPK (p-AMPK) was further confirmed in the livers of mice in the LPS + FGF19 group (Figure 4B).

FGF19 improves LPS-induced oxidative stress and mitochondria dysfunction in vitro

Given the important roles of AMPK activation in bile acids-mediated oxidative stress and mitochondria dysfunction, ROS production and $\Delta\psi$m were detected in HepG2 cells. The ROS production in the LPS + FGF19 group was almost totally blocked compared with the LPS group in HepG2 cells (Figure 5A and B). In addition, the repression of $\Delta\Psi$m was reversed in the LPS + FGF19 group (Figure 5C and D). To further investigate the potential roles of the antioxidative ability of FGF19, an H_2O_2-induced oxidative stress model was used in HepG2 cells. The survival rate of the H_2O_2 + FGF19 group was higher than the H_2O_2 group; it means that the FGF19 pretreatment protected cell viability in response to H_2O_2 stimuli in HepG2 cells (Figure 5E). Consistently, H_2O_2-induced high levels of intracellular ROS, which were totally suppressed in cells that received FGF19 pretreatment (Figure 5F), similar to the results of LPS-induced ROS production shown in Figure 5A.

FGF19 alleviates LPS-induced apoptosis and oxidative stress via activating the AMPK signaling pathway

To confirm the effects of AMPK activation on FGF19-mediated protective effects in response to LPS, CC was used to suppress AMPK activation. CC significantly suppressed the expression of p-AMPK (P=0.0054) (Figure 6A and B) and blocked the improvement of ROS production (Figure 6C) and induction of $\Delta\Psi$m by FGF19 pretreatment (Figure 6D and E).

Discussion

Targeting cholestasis is a potential approach for improving septic liver injury. In the present study, we found that intestine-derived FGF19, which is a regulator of bile acid enterohepatic circulation, was lower in the sera of pediatric patients with sepsis than in healthy children. FGF19 mitigated LPS-induced ALI

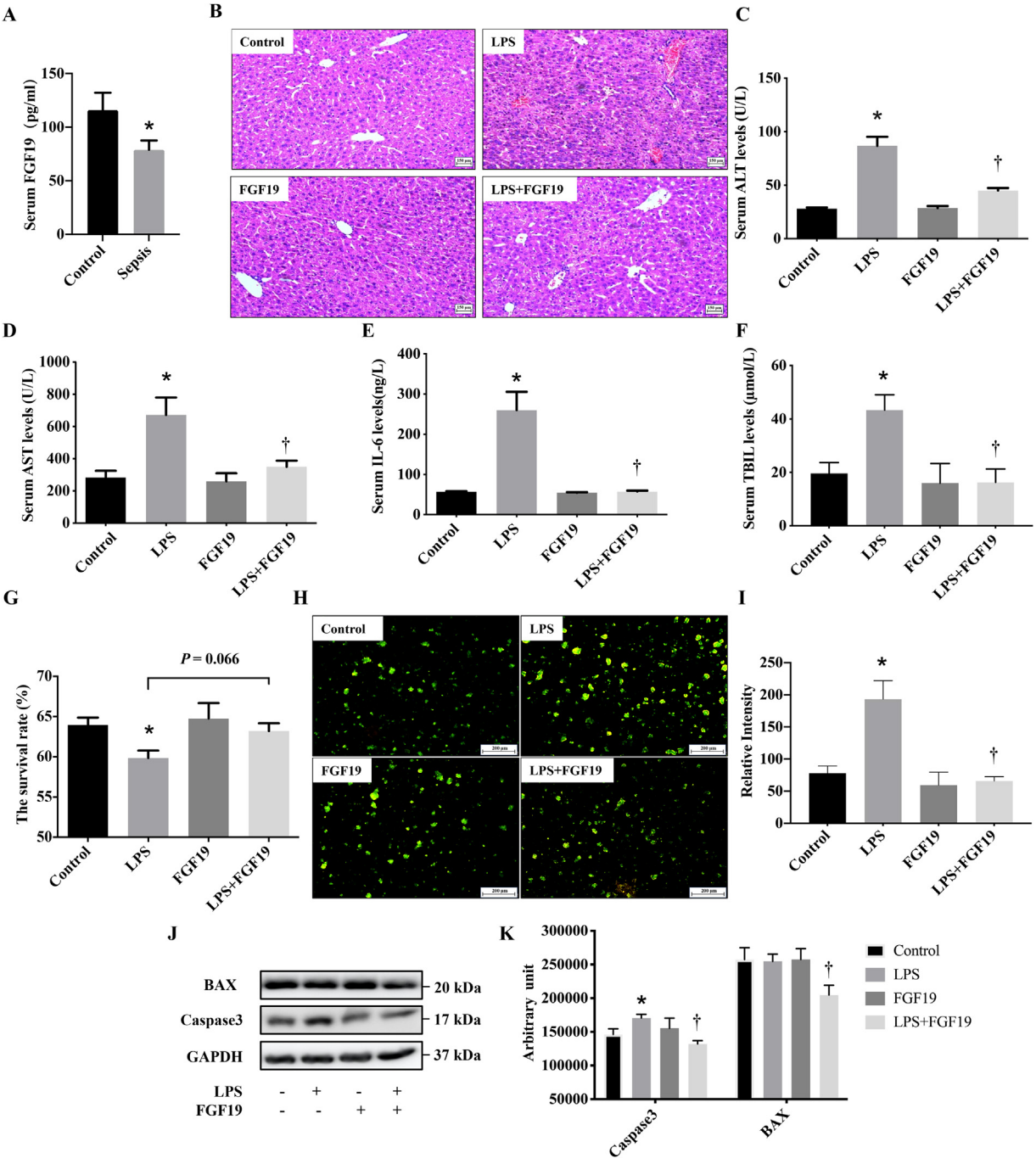

Figure 1. FGF19 exerts a hepatoprotective effect against sepsis-associated acute liver injury. The mice were divided into the four groups (n=6/group). HepG2 cells were treated with FGF19 for 24 h followed by LPS for 8 h (n=3). A: Serum FGF19 levels in healthy control (n = 30) and sepsis pediatric patients (n = 58). B: H&E staining of mice liver sections in different groups. C: Mice serum ALT levels. D: Mice serum AST levels. E: Mice serum IL-6 levels. F: Mice serum TBIL levels. G: The survival rate of HepG2 cells by Corning star Cell counter. H: Apoptosis of HepG2 cells with TUNEL staining. I: The quantitative analysis of TUNEL staining. J: Western blotting for the expression of BAX and Caspase3. K: Quantitative analysis of western blotting.

*indicates the notable difference compared with the Control group, P <0.05.

†indicates the notable difference compared with the LPS group, P <0.05.

ALI: Acute liver injury; ALT: Alanine aminotransferase; AST: Aspartate aminotransferase; FGF19: Fibroblast growth factor 19; H&E: Hematoxylin and eosin; IL-6: Interleukin-6; LPS: Lipopolysaccharide; TBIL: Total bilirubin; TUNEL: TdT-mediated dUTP Nick-End Labeling; BAX: BCL2-Associated X Protein;.

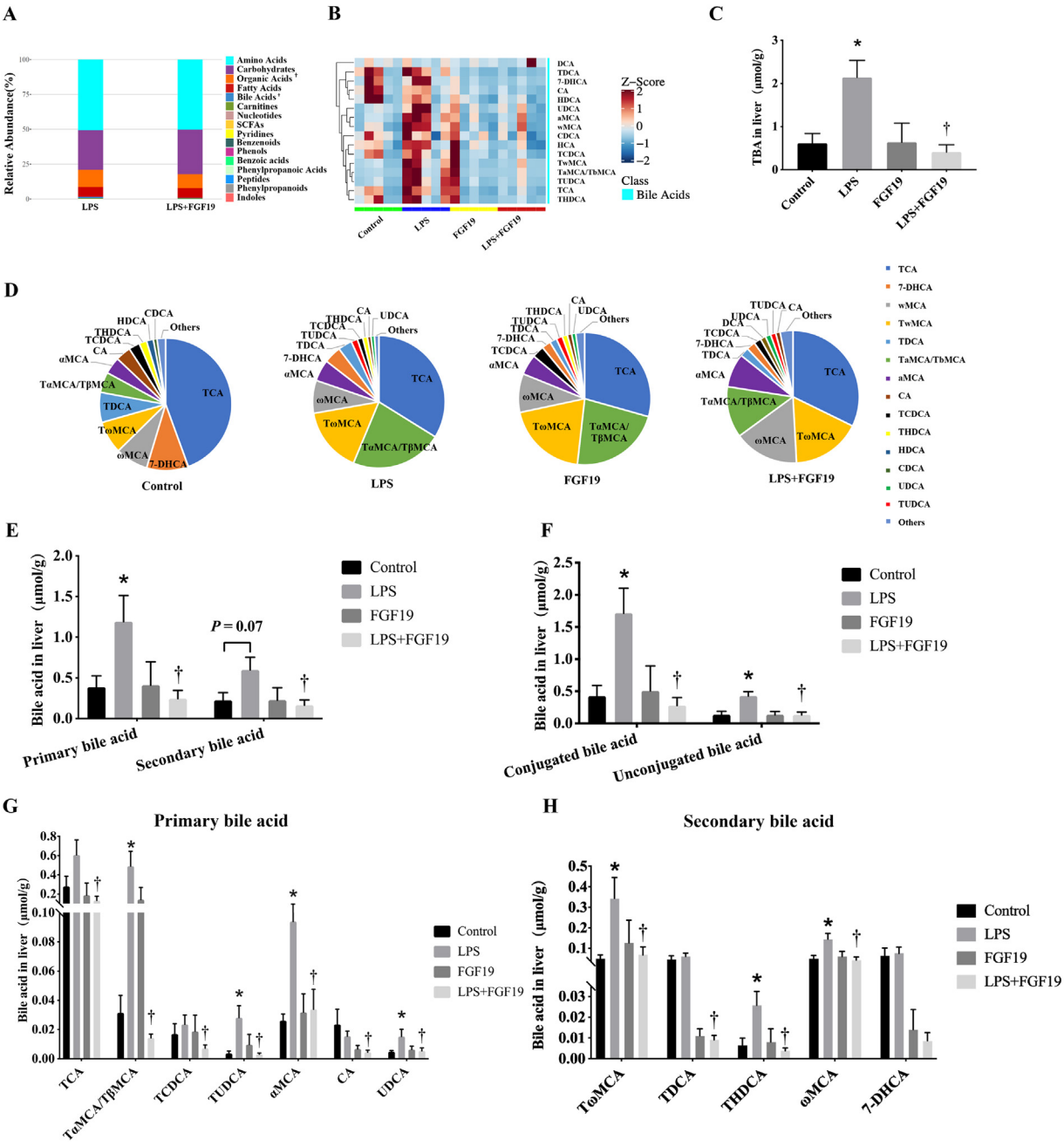

Figure 2. FGF19 improves LPS-induced bile acid homeostasis disorder in mice livers. The mice were divided into the four groups (n=5/group). A: Classification of metabolites. B: Heatmap of bile acids profiles. C: TBA levels in livers. D: Pie chart of bile acids in livers. E: Bar charts of total primary/secondary bile acid. F: Bar charts of total conjugated/unconjugated bile acid. G: Each kind of primary bile acid in liver. H: Each kind of secondary bile acid in liver.
*indicates significant differences compared with Control group, P <0.05.
†indicates significant differences compared with the LPS group, P <0.05.
αMCA: α-muricholic acid; ωMCA: ω-muricholic acid; 7-DHCA: 7-dehydrocholic acid; CA: Cholic acid; CDCA: Chenodeoxycholic acid; DCA: Deoxycholic acid; FGF19: Fibroblast growth factor 19; HCA: Hyocholic acid; HDCA: Hyodeoxycholic acid; LPS: Lipopolysaccharide; TαMCA/TβMCA: Tauro-α-muricholic acid/Tauro-β-muricholic acid; TωMCA: Tauro-ω-muricholic acid; TBA: Total bile acid; TCA: Taurocholic acid; TCDCA: Taurochenodeoxycholic acid; TDCA: Taurodeoxycholic acid; THDCA: Taurohyodeoxycholic acid; TUDCA: Tauroursodeoxycholic acid; UDCA: Ursodeoxycholic acid.

associated with improved bile acid homeostasis and directly enhanced antioxidative capacity via activating the AMPK pathway (Figure 7). This paper plays an important role in revealing the effects of FGF19 on LPS-induced liver injury.

Human FGF19 is an ileal enterocytes-secreted endocrine hormone that mostly regulates glucose and lipid metabolism and bile acid metabolism. In our previous study, daily FGF19 (0.1 mg/kg) treatment for 7 days via the tail vein could improve LPS-induced fatty acid metabolism disorder and organ injury, which are both associated with oxidative stress, mitochondrial function regulation, and ROS generation [18]. In the present study, we focused on the roles and underlying mechanisms by which FGF19 mitigates LPS-induced cholestasis. FGF19 interacts with the hepatic Klotho beta (KLB) co-receptor complexed

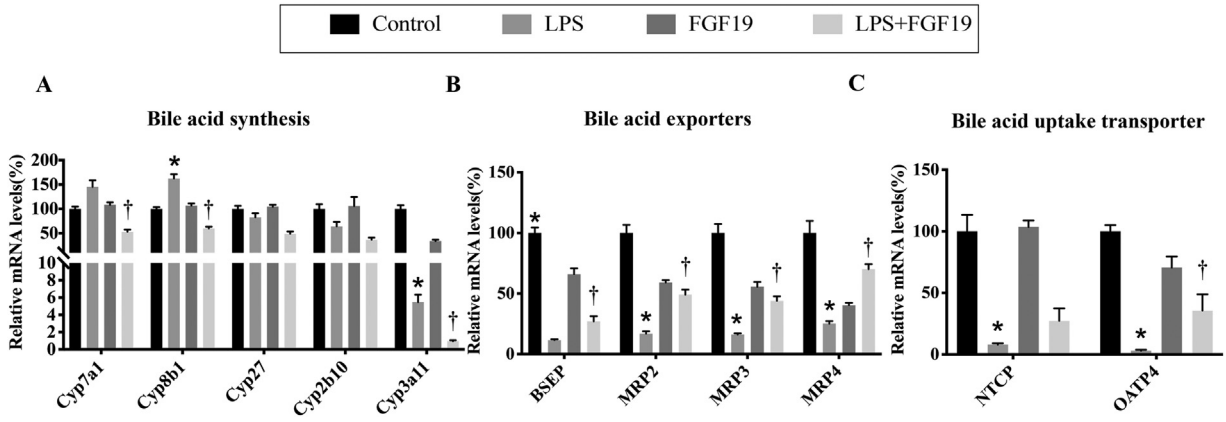

Figure 3. FGF19 reverses the expression of LPS-activated bile acid synthesis and LPS-suppressed apical bile acids and basolateral uptake transporter. The mice were divided into four groups (n=6/group). A: The mRNA expression of genes related to bile acid synthesis in livers. B: The mRNA expression of apical bile acid exporters in livers.C: The mRNA expression of basolateral bile acid uptake transporter.
*indicates significant differences compared with Control group, P <0.05.
†indicates significant differences compared with LPS group, P <0.05.
BSEP: Bile salt export pump; CYP7A1: Cholesterol 7-α-hydroxylase; CYP8B1: Sterol 12α-hydroxylase; CYP27: Cytochrome P450 Family 27; CYP2B10: Cytochrome P450 Family 2 Subfamily B Member 10; CYP3A11: Cytochrome P450 Family 3 Subfamily A Member 11; FGF19: Fibroblast growth factor 19; LPS: Lipopolysaccharide; BSEP: Bile Salt Export Pump; MRP2: Multidrug resistance-associated protein-2; MRP3: Multidrug resistance-associated protein-3; MRP4: Multidrug resistance-associated protein-4; NTCP: Sodium taurocholate co-transporting polypeptide; OATP4: Organic anion transporting polypeptide-4.

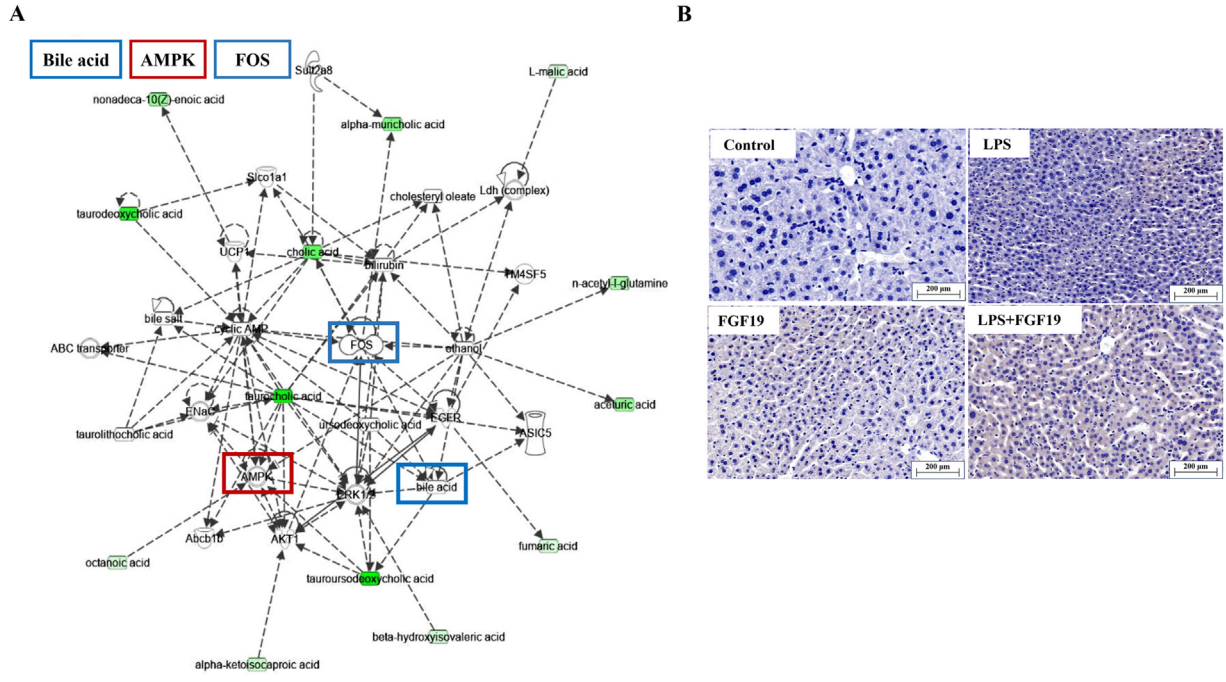

Figure 4. FGF19 alleviates LPS-induced hepatocytes apoptosis associated with AMPK activation *in vivo* and *in vitro*. The mice were divided into the four groups (n=6/group). A: IPA integrated analysis of metabolomic data (n=5). B: Immunohistochemical analysis for the expression of p-AMPK in livers.
ABC transporter: ATP-binding cassette transporter; AKT1: RAC-alpha serine/threonine-protein kinase; AMPK: AMP-activated protein kinase; AP-1: Activator Protein 1; ASIC5: Acid-sensing ion channel 5; EGFR: Epidermal Growth Factor Receptor; FGF19: Fibroblast growth factor 19; *FOS*: Fos proto-oncogene, AP-1 transcription factor subunit; IPA: Ingenuity pathways analysis; LPS: Lipopolysaccharide; p-AMPK: Phosphorylated AMPK.

with FGFR4 kinase to regulate bile acid metabolism.[19] In this study, we reported that FGF19 pretreatment could inhibit the LPS-induced bile acid synthesis and export in liver via maintaining the intestine–liver crosstalk bile acid homeostasis. Whether FGF19 binds to FGFR4 needs further study in the future. FGF19 also directly activates AMPK to alleviate LPS-induced oxidative stress in hepatocytes. Intraperitoneal daily injection of recombinant FGF19 (0.1 mg/kg) for three consecutive weeks could improve muscle loss and partial grip strength in obese mice through the AMPK signaling pathway,[20] thus suggesting that AMPK could be the main downstream signaling intermediate of FGF19.

In this study, circulating FGF19 levels in children with sepsis were lower than those in healthy children. The difference between patients with or without liver injury needs investigation in a larger population. In rhesus monkeys, anti-FGF19 antibody

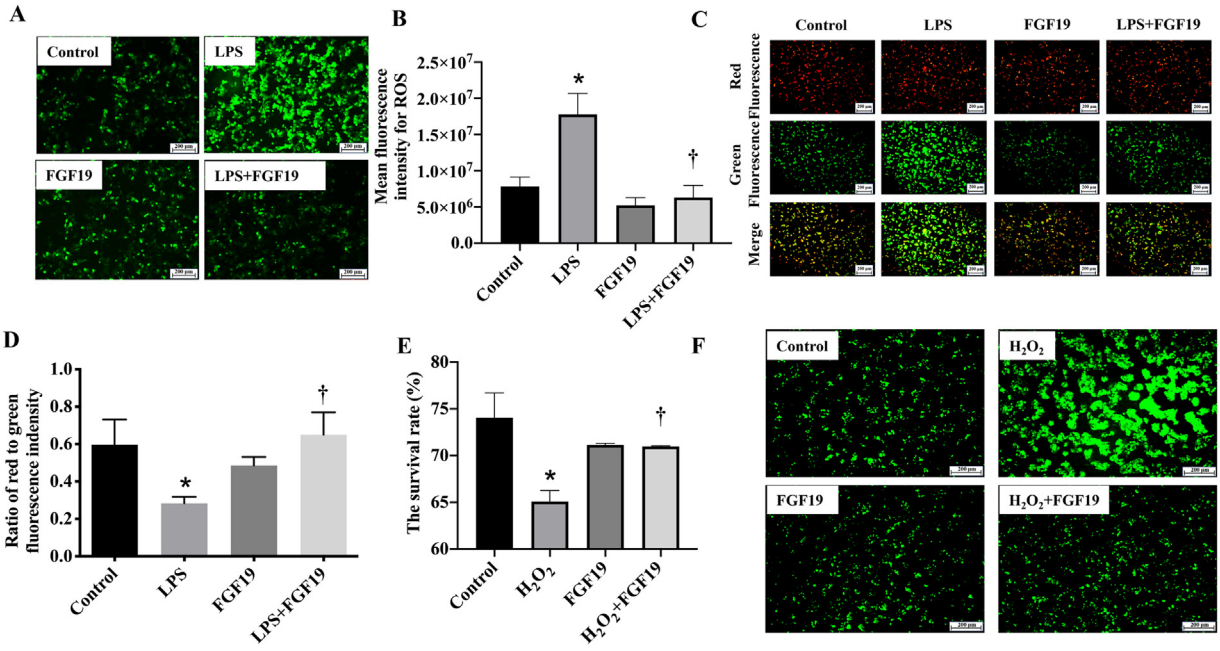

Figure 5. FGF19 improves oxidative stress and mitochondrial dysfunction in response to LPS or H_2O_2. HepG2 cells were treated with FGF19 for 24 h followed by LPS for 8 h (n=3) (A–D), and HepG2 cells were treated with FGF19 for 24 h followed by H_2O_2 for 2 h (n=3) (E and F). A: Representative images of ROS in response to LPS.B: The quantitative analysis of ROS production.C: The determination of ΔΨm by JC-1 staining.D:The quantitative analysis of JC-1 staining.E: The survival rate.F: Representative images of ROS in response to H_2O_2.

*indicates the notable difference compared with Control group, P <0.05.

†indicates the notable difference compared with LPS or H_2O_2 group, P <0.05.

FGF19: Fibroblast growth factor 19; LPS: Lipopolysaccharide; ROS: Reactive oxygen species.

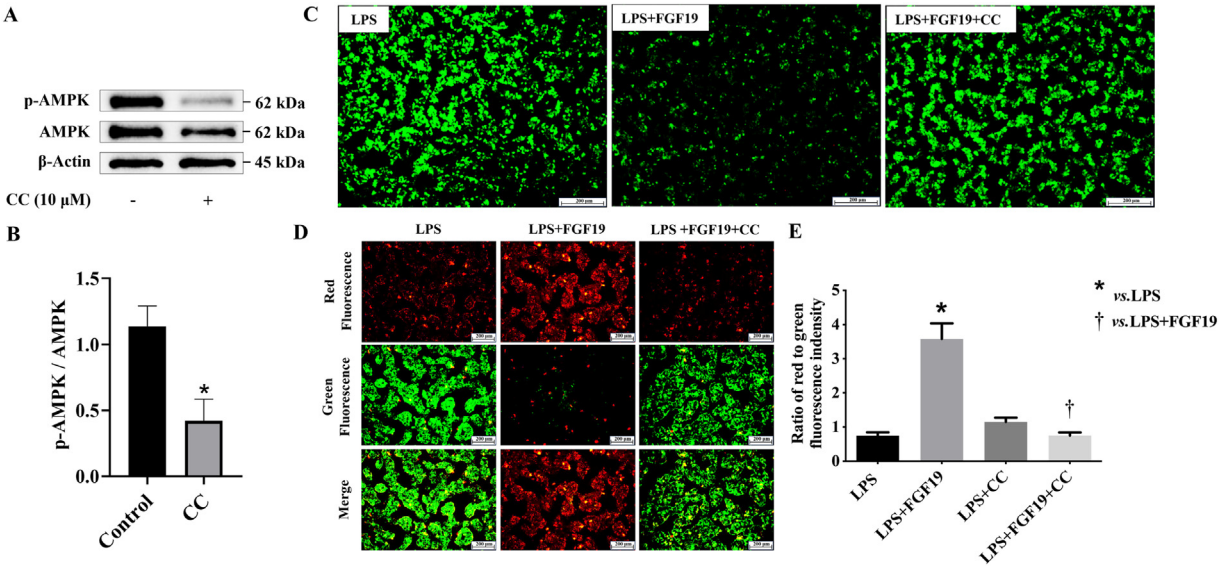

Figure 6. FGF19 alleviates LPS-induced oxidative stress and mitochondrial dysfunction via AMPK activation. HepG2 cells were treated with CC (10 μmol/L) for 2 h (n=3) (A). Then treated with FGF19 for 24 h followed by LPS for 8 h (n = 3) (B–D). A: Western blotting analysis of the total and phosphorylated protein levels of AMPK. B: The P-AMPK/AMPK quantitative analysis of Western blotting.C: Representative images of ROS.D: The determination of ΔΨm by JC-1 staining.E: The quantitative analysis of JC-1 staining.

*indicates significant differences compared with Control (B) or LPS (E) group, P <0.05.

†indicates significant differences compared with LPS + FGF19 group, P <0.05.

AMPK: AMP-activated protein kinase; CC: Compound C; FGF19: Fibroblast growth factor 19; LPS: Lipopolysaccharide; p-AMPK: Phosphorylated AMPK; ROS: Reactive oxygen species.

induces increased bile acid synthesis, and changes in the bile acid transporters expression in the liver and ileum result in enterohepatic recirculation of bile acids.[21] In addition, aldafermin (also known as NGM282 or M70) is an engineered, non-tumorigenic analog of the human gut hormone FGF19. Clinical trials have proven that a 12-week or 24-week treatment regimen with aldafermin improves the histological features of non-alcoholic steatohepatitis (NASH).[22,23] Evidence has shown that a decrease in circulating FGF19 concentrations is associated with an elevation in bile acid levels in NASH patients.[16,24]

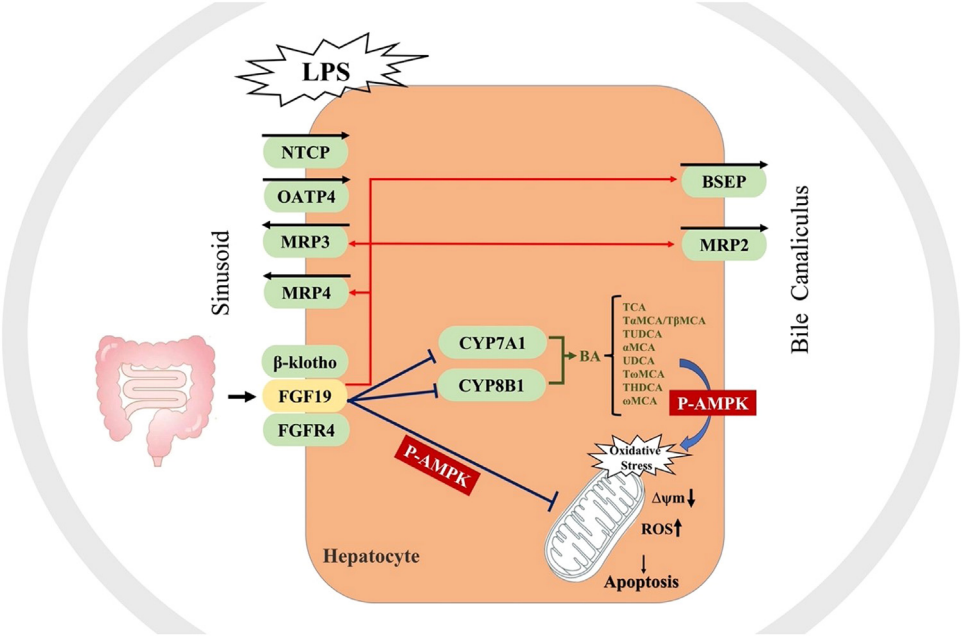

Figure 7. FGF19 working model. Intestine-derived FGF19 enters the liver via the portal vein, and FGF19 possibly binds to β-Klotho and FGFR4 on the membrane of hepatocytes, consequently inhibiting the expression of CYP7A1 and CYP8B1 to suppress the bile acid synthesis. During sepsis or in response to LPS, decreased FGF19 leads to failure in feedback of bile acid synthesis and exportation resulting in bile acids accumulation in hepatocytes, which induces oxidative stress-induced decreased ΔΨm and ROS overproduction. In addition to the role of FGF19 in maintaining bile acid homeostasis, FGF19 can directly resist LPS-induced mitochondrial dysfunction and ROS production via activating the AMPK signaling pathway in hepatocytes.
αMCA: α-muricholic acid; ωMCA: ω-muricholic acid; AMPK: AMP-activated protein kinase; BSEP: Bile salt export pump; CYP7A1: Cholesterol 7-α-hydroxylase; CYP8B1: Sterol 12α-hydroxylase; FGF19: Fibroblast growth factor 19; FGFR4: Fibroblast growth factor receptor 4; LPS: Lipopolysaccharide; MRP2: Multidrug resistance-associated protein-2; MRP3: Multidrug resistance-associated protein-3; MRP4: Multidrug resistance-associated protein-4; NTCP: Sodium taurocholate co-transporting polypeptide; OATP4: Organic anion transporting polypeptide-4; p-AMPK: Phosphorylated AMPK; ROS: Reactive oxygen species; TαMCA: Tauro-α-muricholic acid; TβMCA: Tauro-β-muricholic acid; TωMCA: Tauro-ω-muricholic acid; TCA: Taurocholic acid; THDCA: Taurohyodeoxycholic acid; TUDCA: Tauroursodeoxycholic acid; UDCA: Ursodeoxycholic acid.

Importantly, aldafermin suppresses the synthesis of bile acids and, in particular, decreases the content of toxic bile acids.[25] In our study, FGF19 pretreatment reverses LPS-induced severe cholestasis and liver damage in mice. Thus, we speculated that FGF19 has the potential to become a new therapeutic target for SALI.

In patients with Crohn's disease, the FGF19 signaling pathway regulates the size and composition of bile acid pools by inhibiting the expression of CYP7A1.[26] Both FGF19 and its analogs M70 inhibited the expression of CYP7A1 and CYP27A1, thereby reversing liver damage and relieving liver inflammation in a model of extensive bile duct disease.[27] Consistently, FGF19 not only suppresses the expression of CYP7A1, CYP27, and CYP8B1 in livers but also regulates the expression of bile acid efflux-related genes such as *BSEP, MRP2, MRP3,* and *MRP4*. Therefore, we infer that FGF19 not only inhibits bile acid synthesis but also promotes bile acid efflux to improve LPS-induced cholestasis, thereby relieving LPS-induced ALI.

ROS play a crucial role in bile acid-induced oxidative stress. Although ROS is mainly released by mitochondria, excessive ROS will cause damage to the mitochondria itself. Normal $\Delta\psi$m is indispensable for maintaining mitochondrial function. Reduced $\Delta\psi$m will promote mitochondrial dysfunction and induce cell apoptosis.[28,29] In the case of diabetic cardiomyopathy, FGF19 induces an antioxidant response by stimulating the expression of nuclear factor erythroid 2-related factor 2 (Nrf2) and reducing the production of ROS.[30] Overexpression of FGF19 alleviates hypoxia/reoxygenation-induced damage of cardiomyocytes by regulating glycogen synthase kinase-3β (GSK-3β)/Nrf2/antioxidant response elemen (ARE) signaling.[31] In the present study, FGF19 reverses LPS-indued $\Delta\psi$m reduction and excessive ROS production and alleviates LPS-induced oxidative stress in livers and hepatocytes. We further confirmed that the antioxidant capacity of FGF19 might depend on bile acid metabolism pathways *in vivo* or may have a direct regulatory effect on mitochondrial function via activating the AMPK signaling pathway.

Conclusions

FGF19 is associated with the occurrence of sepsis in children. FGF19 pretreatment ameliorates LPS-induced ALI in mice. Mechanically, FGF19 not only maintains bile acid homeostasis in response to LPS in the liver but also directly improves LPS-indu ced oxidative stress in hepatocytes. These findings provide new insights for the targeting of cholestasis as a potential therapy against SALI, and FGF19 – an intestine-derived small molecule – might be a remarkable therapeutic target for SALI treatment.

CRediT Authorship Contribution Statement

Xiaomeng Tang: Writing – original draft, Visualization, Validation, Software, Formal analysis. **Jingjing Ning:** Investigation, Validation, Visualization. **Yilin Zhao:** Visualization, Validation. **Shuyun Feng:** Validation. **Lujing Shao:** Validation. **Tiantian Liu:** Formal analysis. **Huijie Miao:** Resources,

Data curation. **Yucai Zhang:** Investigation, Funding acquisition. **Chunxia Wang:** Writing – review & editing, Supervision, Methodology, Funding acquisition, Conceptualization. All authors read and approved the final manuscript.

Acknowledgment

None.

Funding

This work was supported by the National Natural Science Foundation of China (grant number: 82171729); the Natural Science Foundation of Shanghai (grant number: 23ZR1453000); the Shanghai Municipal Health Commission (grant number: 202340076); and the Shanghai Municipal Education Commission-Gaofeng Clinical Medicine Grant (grant number: 20171928).

Ethics Statement

The study protocol was approved by the local ethics committee and conducted in accordance with the ethical standards laid down in the Declaration of Helsinki (Ethics Committee of Children's Hospital affiliated to Shanghai Jiao Tong university; approval number: 2018R039-F01). The informed consent was signed by the patients' legal authorized guardian. Detailed methods are described in Supplementary Material.

Conflict of Interest

The authors declare no potential conflicts of interest with respect to the research, authorship, and/or publication of this article.

Data Availability

The datasets generated and analyzed during the current study are available from the corresponding author on reasonable request.

Supplementary Materials

Supplementary material associated with this article can be found, in the online version, at doi:10.1016/j.jointm.2024.06.003.

References

[1] Singer M, Deutschman CS, Seymour CW, Shankar-Hari M, Annane D, Bauer M, et al. The third international consensus definitions for sepsis and septic shock (sepsis-3). JAMA 2016;315:801–10. doi:10.1001/jama.2016.0287.
[2] Strnad P, Tacke F, Koch A, Trautwein C. Liver – guardian, modifier and target of sepsis. Nat Rev Gastroenterol Hepatol 2017;14:55–66. doi:10.1038/nrgastro.2016.168.
[3] Wei S, Ma X, Zhao Y. Mechanism of hydrophobic bile acid-induced hepatocyte injury and drug discovery. Front Pharmacol 2020;11:1084. doi:10.3389/fphar.2020.01084.
[4] Berg RD. Bacterial translocation from the gastrointestinal tract. J Med 1992;23:217–44.
[5] Ding JW, Andersson R, Soltesz V, Willén R, Bengmark S. The role of bile and bile acids in bacterial translocation in obstructive jaundice in rats. Eur Surg Res 1993;25:11–19. doi:10.1159/000129252.
[6] Chambers KF, Day PE, Aboufarrag HT, Kroon PA. Polyphenol effects on cholesterol metabolism via bile acid biosynthesis, CYP7A1: a review. Nutrients 2019;11:2588. doi:10.3390/nu11112588.
[7] Kim I, Ahn SH, Inagaki T, Choi M, Ito S, Guo GL, et al. Differential regulation of bile acid homeo-stasis by the farnesoid X receptor in liver and intestine. J Lipid Res 2007;48:2664–72. doi:10.1194/jlr.M700330-JLR200.
[8] Inagaki T, Choi M, Moschetta A, Peng L, Cummins CL, McDonald JG, et al. Fibroblast growth factor 15 functions as an enterohepatic signal to regulate bile acid homeostasis. Cell Metab 2005;2:217–25. doi:10.1016/j.cmet.2005.09.001.
[9] Jenniskens M, Langouche L, Vanwijngaerden YM, Mesotten D, Van den Berghe G. Cholestatic liver (dys)function during sepsis and other critical illnesses. Intensive Care Med 2016;42:16–27. doi:10.1007/s00134-015-4054-0.
[10] Mutanen A, Lohi J, Heikkilä P, Jalanko H, Pakarinen MP. Loss of ileum decreases serum fibroblast growth factor 19 in relation to liver inflammation and fibrosis in pediatric onset intestinal failure. J Hepatol 2015;62:1391–7. doi:10.1016/j.jhep.2015.01.004.
[11] Pastor A, Collado PS, Almar M, González-Gallego J. Antioxidant enzyme status in biliary obstructed rats: effects of N-acetylcysteine. J Hepatol 1997;27:363–70. doi:10.1016/S0168-8278(97)80183-3.
[12] Vendemiale G, Grattagliano I, Lupo L, Memeo V, Altomare E. Hepatic oxidative alterations in patients with extra-hepatic cholestasis. Effect of surgical drainage. J Hepatol 2002;37:601–5. doi:10.1016/S0168-8278(02)00234-9.
[13] Jaeschke H. Mechanisms of liver injury. II. Mechanisms of neutrophil-induced liver cell injury during hepatic ischemia-reperfusion and other acute inflammatory conditions. Am J Physiol Gastrointest Liver Physiol 2006;290:G1083–8. doi:10.1152/ajpgi.00568.2005.
[14] Gujral JS, Liu J, Farhood A, Jaeschke H. Reduced oncotic necrosis in Fas receptor-deficient C57BL/6J-lpr mice after bile duct ligation. Hepatology 2004;40:998–1007. doi:10.1002/hep.1840400431.
[15] Guo A, Li K, Xiao Q. Fibroblast growth factor 19 alleviates palmitic acid-induced mitochondrial dysfunction and oxidative stress via the AMPK/PGC-1alpha pathway in skeletal muscle. Biochem Biophys Res Commun 2020;526:1069–76. doi:10.1016/j.bbrc.2020.04.002.
[16] Puri P, Daita K, Joyce A, Mirshahi F, Santhekadur PK, Cazanave S, et al. The presence and severity of nonalcoholic steatohepatitis is associated with specific changes in circulating bile acids. Hepatology 2018;67:534–48. doi:10.1002/hep.29359.
[17] Uchiyama K, Naito Y, Takagi T, Mizushima K, Hayashi N, Handa O, et al. FGF19 protects colonic epithelial cells against hydrogen peroxide. Digestion 2011;83:180–3. doi:10.1159/000321809.
[18] Liu T, Tang X, Cui Y, Xiong X, Xu Y, Hu S, et al. Fibroblast growth factor 19 improves LPS-induced lipid disorder and organ injury by regulating metabolomic characteristics in mice. Oxid Med Cell Longev 2022;2022:9673512. doi:10.1155/2022/9673512.
[19] Li X, Lu W, Kharitonenkov A, Luo Y. Targeting the FGF19-FGFR4 pathway for cholestatic, metabolic, and cancerous diseases. J Intern Med 2024;295:292–312. doi:10.1111/joim.13767.
[20] Guo A, Li K, Tian HC, Fan Z, Chen QN, Yang YF, et al. FGF19 protects skeletal muscle against obesity-induced muscle atrophy, metabolic derangement and abnormal irisin levels via the AMPK/SIRT-1/PGC-α pathway. J Cell Mol Med 2021;25:3585–600. doi:10.1111/jcmm.16448.
[21] Pai R, French D, Ma N, Hotzel K, Plise E, Salphati L, et al. Antibody-mediated inhibition of fibroblast growth factor 19 results in increased bile acids synthesis and ileal malabsorption of bile acids in cynomolgus monkeys. Toxicol Sci 2012;126:446–56. doi:10.1093/toxsci/kfs011.
[22] Harrison SA, Rossi SJ, Paredes AH, Trotter JF, Bashir MR, Guy CD, et al. NGM282 improves liver fibrosis and histology in 12 weeks in patients with nonalcoholic steatohepatitis. Hepatology 2020;71:1198–212. doi:10.1002/hep.30590.
[23] Harrison SA, Neff G, Guy CD, Bashir MR, Paredes AH, Frias JP, et al. Efficacy and safety of aldafermin, an engineered FGF19 analog, in a randomized, double-blind, placebo-controlled trial of patients with nonalcoholic steatohepatitis. Gastroenterology 2021;160:219–31 e1. doi:10.1053/j.gastro.2020.08.004.
[24] Caussy C, Hsu C, Singh S, Bassirian S, Kolar J, Faulkner C, et al. Serum bile acid patterns are associated with the presence of NAFLD in twins, and dose-dependent changes with increase in fibrosis stage in patients with biopsy-proven NAFLD. Aliment Pharmacol Ther 2019;49:183–93. doi:10.1111/apt.15035.
[25] Loomba R, Ling L, Dinh DM, DePaoli AM, Lieu HD, Harrison SA, et al. The commensal microbe veillonella as a marker for response to an FGF19 analog in NASH. Hepatology 2021;73:126–43. doi:10.1002/hep.31523.
[26] Gadaleta RM, Garcia-Irigoyen O, Cariello M, Scialpi N, Peres C, Vetrano S, et al. Fibroblast growth factor 19 modulates intestinal microbiota and inflammation in presence of Farnesoid X receptor. EBioMedicine 2020;54:102719. doi:10.1016/j.ebiom.2020.102719.
[27] Zhou M, Learned RM, Rossi SJ, DePaoli AM, Tian H, Ling L. Engineered fibroblast growth factor 19 reduces liver injury and resolves sclerosing cholangitis in Mdr2-deficient mice. Hepatology 2016;63:914–29. doi:10.1002/hep.28257.
[28] Wang GY, Zhang JW, Lü QH, Xu RZ, Dong QH. Berbamine induces apoptosis in human hepatoma cell line SMMC7721 by loss in mitochondrial transmembrane potential and caspase activation. J Zhejiang Univ Sci B 2007;8:248–55. doi:10.1631/jzus.2007.B0248.
[29] Nazim UM, Yin H, Park SY. Autophagy flux inhibition mediated by celastrol sensitized lung cancer cells to TRAIL-induced apoptosis via regulation of mitochondrial transmembrane potential and reactive oxygen species. Mol Med Rep 2019;19:984–93. doi:10.3892/mmr.2018.9757.
[30] Li X, Wu D, Tian Y. Fibroblast growth factor 19 protects the heart from oxidative stress-induced diabetic cardiomyopathy via activation of AMPK/Nrf2/HO-1 pathway. Biochem Biophys Res Commun 2018;502:62–8. doi:10.1016/j.bbrc.2018.05.121.
[31] Fang Y, Zhao Y, He S, Guo T, Song Q, Guo N, et al. Overexpression of FGF19 alleviates hypoxia/reoxygenation-induced injury of cardiomyocytes by regulating GSK-3beta/Nrf2/ARE signaling. Biochem Biophys Res Commun 2018;503:2355–62. doi:10.1016/j.bbrc.2018.06.161.